Ships and Offshore Structures

ISSN: (Print) (Online) Journal homepage: https://www.tandfonline.com/loi/tsos20

On the effects of the number of baffles in sloshing dynamics

Fatih C. Korkmaz & Bülent Güzel

To cite this article: Fatih C. Korkmaz & Bülent Güzel (2023) On the effects of the number of baffles in sloshing dynamics, Ships and Offshore Structures, 18:1, 21-33, DOI: 10.1080/17445302.2021.2007676

To link to this article: https://doi.org/10.1080/17445302.2021.2007676

Published online: 04 Dec 2021.

SHIPS AND OFFSHORE STRUCTURES
2023, VOL. 18, NO. 1, 21–33
https://doi.org/10.1080/17445302.2021.2007676

Taylor & Francis
Taylor & Francis Group

On the effects of the number of baffles in sloshing dynamics

Fatih C. Korkmaz [a] and Bülent Güzel [b]

[a]Department of Marine Engineering Operations, Yildiz Technical University, Istanbul, Turkey; [b]Department of Mechatronics Engineering, Istanbul Gelisim University, Istanbul, Turkey

ABSTRACT

This study examines the effect of the number of perforated baffles in sloshing phenomenon in a partially filled tank. The natural frequencies in one-, two- and no-baffle cases are experimentally obtained; change in natural frequencies and reduction in sloshing impacts due to baffles are reported. It is observed that adding the second baffle has a minor effect in damping the sloshing loads at non-resonance frequencies in comparison to ones obtained in one-baffle sloshing tests. Although the natural frequency is significantly increased and pressure distribution profile is altered at higher oscillation frequencies in two-baffle case, the significant reduction in peak pressure values is observed at the frequencies near the natural frequency in one-baffle case. The results indicate that the number of the baffles should be optimised considering the natural frequency of the carrier and external excitation frequencies for the purpose of weight minimisation, fast loading and unloading of the tanks.

ARTICLE HISTORY
Received 5 March 2021
Accepted 14 November 2021

KEYWORDS
Sloshing; perforated baffles; wave impact; surging

1. Introduction

Sloshing is encountered in moving platforms carrying partially liquid-filled containers (e.g. tanker trucks and tanker ships) and resulted from an external excitation. Therefore, the prediction of the impact loads due to sloshing and the suppression of these loads are of great importance in various industrial fields such as marine, aerospace, civil and transportation industries. This phenomenon causes violent fluid motions and additional accelerations that result in free surface deformations and high impact pressures on tank walls, which may later lead to structural damage of the tank walls and/or instabilities of the moving platforms. Based on various parameters, e.g. magnitude and frequency of the excitation, fluid height and tank length, different types of wave impacts may occur in tanks, i.e. standing wave or broken wave impacts. This difference in wave characteristics can alter the impact characteristics (Lugni et al. 2006).

In the maritime industry, sloshing not only affects the stability of a vessel but also influences the seakeeping strategy of a vessel in regards with hull motions under sloshing effects, e.g. side-to-side movement of liquid cargo in a ship may lead to listing due to shifted weight causing delayed arrival times. In this regard, numerous experimental, analytical and numerical investigations on sloshing phenomenon have been carried out. Sway or roll motion is preferred for excitation in experimental studies. The potential flow theory or a viscous fluid model based on solving Navier–Stokes equations is widely used in numerical studies. Hattori et al. (1994) studied the impact characteristics of waves when hitting on vertical walls. They observed that the trapped air that occurs during an impact can change the impact pressure and its time history. Wood et al. (2000) studied the effects of trapped air on wave impacts using the pressure impulse theory. Colagrossi et al. (2004) studied the sloshing phenomenon experimentally and observed the effects of fluid height level in tanks. They monitored the free surface motions and measured the impact loads at different excitation levels. Lugni et al. (2006) experimentally analysed the flip-through events. Bullock et al. (2007) investigated the wave impacts on vertical and inclined walls. Rajasekaran et al. (2010) studied the wave impacts on vertical walls and presented the time history of rising pressures in breaking waves. Lugni et al. (2010a) carried out an experimental investigation of wave impacts in depressurised ambient air conditions. Lugni et al. (2010b) also showed the dynamic features of these wave impacts. Pistani and Thiagarajan (2012) studied sloshing experimentally by inducing sway motions in a rectangular tank and measured the impact pressures. They observed various types of impacts and discussed their effects. Kisacik et al. (2012) studied the wave impacts on horizontal cantilevering slabs with vertical structures. They measured the pressures on the vertical and top sections, and determined their peak points. Bouscasse et al. (2013) experimentally investigated the shallow water cases of sloshing. They applied the δ-SPH model in violent sloshing cases to capture the wave elevations. Song et al. (2013) experimentally studied sloshing in partially filled rectangular tanks and investigated the wave impacts on vertical walls. Zou et al. (2015) studied the viscosity effects in sloshing. They showed that in highly viscous fluids, less impact forces on the sidewalls are observed due to energy dissipation caused by the viscous friction. Souto-Iglesias et al. (2015) used various tanks under harmonic excitation in their experiments to investigate the role of tank width in sloshing phenomenon and the peak pressure values. Kim et al. (2017) experimentally investigated the scale effect in sloshing and reported that the location of maximum pressure varies depending on the scale size. Tosun et al. (2017) used an image processing technique in order to estimate the sloshing forces by tracking the free surface deformations. Lu et al. (2018) conducted a series of experiments to study the effects of fill level in sloshing. Their study showed that the amplitude is inversely proportional to the fill level, i.e. the amplitude decreases with increasing fill level. Xue et al. (2019) numerically investigated the sloshing dynamics in various shaped tanks with matching fluid volumes. They demonstrated that significantly lower sloshing effects are observed in chamfer-shaped tanks compared to the other tank shapes. Shamsoddini and Abolpur (2021) carried numerical simulations to investigate the sloshing phenomenon in Bingham fluids i.e. a non-Newtonian fluid.

CONTACT Fatih C. Korkmaz fkorkmaz@yildiz.edu.tr

Free surface deformations and fluid movements during a sloshing event can be suppressed or limited by various methods. Recently, Sauret et al. (2015) showed that damping out the oscillations of the free surface may be realised by adding foam into the void of a partially filled tank. The foam can alter the fluid dynamics in the tank significantly and reduce the amplitude of movements. Many researchers have utilised solid or perforated baffles with different shapes and arrangements in their experimental or numerical tanks in order to suppress the sloshing effects. Most of these studies focused on damping properties of baffles under free oscillations or harmonic/single-cycle sinusoidal excitations (Xue et al. 2017). Akyildiz and Ünal (2005) carried out experiments on the three-dimensionality effects of sloshing loads via pressure distributions. They also considered the cases with baffles and reported that some mitigation of fluid motion is observed when using baffles, i.e. damping the sloshing loads. Maleki and Ziyaeifar (2008) studied sloshing in a cylindrical tank with baffles. They considered various configurations of baffles and showed the higher effectiveness of the ring-type baffles in mitigating the fluid motion. Nasar et al. (2008) carried out pressure measurements on the tank walls to investigate the effects of wave amplitudes and excitation frequencies on sloshing loads. Liu and Lin (2009) conducted two- and three-dimensional sloshing tests in a tank with vertical baffles. Goudarzi et al. (2010) carried out experimental and numerical investigations on sloshing using a rectangular tank with baffles. Various positions of baffles with different dimensions had been considered to investigate the effect of baffles in hydrodynamic damping. They also developed an analytical model to be used in estimating the damping ratio of baffles during earthquake motions. Faltinsen and Timokha (2011) analytically calculated the natural frequencies of rectangular tanks with slotted baffles. Crowley and Porter (2012a) numerically studied the energy dissipation in sloshing when using perforated baffles. Brizzolara et al. (2011) utilised a numerical method to capture the sloshing dynamics and compared their results with the experimental ones. They derived the governing equations by considering the linearised water wave theory and then provided the optimum configuration of baffles in damping the fluid motions. Crowley and Porter (2012b) conducted an analytical investigation on the effects of single thin perforated baffle on wave propagation. Wu et al. (2013) showed the change of natural frequency after installing baffles. Wei et al. (2015) studied the shallow water regime in sloshing using a rectangular tank with perforated baffles of various solidity ratios. They proposed an optimal slat ratio in overcoming the sloshing loads. They also reported that the baffles can shift the sloshing resonance frequency. Cho and Kim (2016) analytically and experimentally investigated the double vertical perforated baffle effects on sloshing loads in rectangular tanks. Their results showed that dual baffles with optimum solidity ratios are able to overcome sloshing loads significantly. Yu et al. (2017) experimentally and numerically studied the sloshing phenomenon for a liquefied natural gas (LNG) tank with floating membranous plates. They showed that these suppression elements can reduce the impact loads and wave run-ups significantly at various fill levels. Graczyk et al. (2007) studied the sloshing loads on LNG membrane tank. Shamsoddini and Abolpur (2019) applied the incompressible Smoothed Particle Hydrodynamics (ISPH) method to show the effects of baffles in sloshing and demonstrated their role in damping the sloshing fluctuations. Yu et al. (2019) experimentally investigated the effects of perforated baffles with various solidity ratios in damping the sloshing impacts. Bellezi et al. (2019) conducted a series of experiments with a box-shaped tank and a perforated baffle set. The fully Lagrangian particle-based method is used to capture the free surface motions in their numerical studies. Nasar et al. (2021) carried out sloshing experiments and reported the effectiveness of baffles in damping the fluid motion.

When it comes to marine industry, horizontal and vertical anti-slosh baffles are already commonly used in ships in order to prevent excessive pressure on tank walls by damping out the energy of moving fluid. However, the effectiveness of baffles in suppressing longitudinal and lateral liquid slosh strongly depends on some design parameters of the baffles, e.g. location, installation position and orientation of the baffles and their geometrical characteristics (shape, size, perforations). These baffles increase the weight of ships and may interfere with loading/unloading and cleaning processes. Therefore, the number of baffles and their orientation should be optimised for both increased damping effectiveness and reduced baffle weight, with considering the natural frequency of the carrier and possible external excitation frequencies. The main objective of this study is to investigate the effect of the number of perforated baffles in mitigating the sloshing energy and changing the natural frequency of tanks. The damping characteristics of sloshing loads in a partially filled narrow tank with different number of baffles were analysed and compared via free surface deformations and pressure distributions on the side wall. The relative anti-slosh effectiveness of the baffle number is evaluated in terms of pressure-time histories and their peak values for no-baffle, single and double baffle cases. From the results of this study, it is reported that the number of baffles to be installed on a liquid cargo ship can be minimised while performing the necessary amount of damping depending on the excitation frequency and the natural frequency of a ship.

2. Experimental setup

The amplitude of sloshing is a function of liquid level, liquid properties, tank geometry and its motion characteristics, i.e. amplitude and frequency. The current experimental study investigates the damping effects of perforated baffles in sloshing in a narrow rectangular tank subject to surge excitation. Since the impact pressure caused by sloshing in a tank is a function of fill level and the frequency of excitation, experiments were conducted at various tank fill levels and excitation frequencies. A rectangular transparent tank with dimensions of 0.36, 0.4, and 0.07 m is constructed from plexiglass sheets with a thickness of 5 mm (Figure 1). The width of the tank is chosen as 7 cm to eliminate the three-dimensional effects. The top of the tank is also closed to prevent splashing out of the tank during violent sloshing, so that the mass of initial bulk water remains constant. A slot (6×8 cm) is opened on the top plate of the tank to maintain the atmospheric pressure conditions. The tank is mounted on a table that can be excited with sway motions via an AC motor. The speed of the AC motor is controlled with an integrated frequency inverter. Slosh-induced impact pressures were measured on the sidewalls using pressure sensors mounted at different heights. Three pressure sensors (PCM300D model by SHLLJ) with a measuring range of up to 0.4 bar, a precision of 0.5%, a response time of 20 μs (50kHz) and a diaphragm diameter of 3.5 mm are mounted on the side wall with a spacing of 5 cm positioned from the bottom plate as illustrated in Figure 1. Hioki LR8400 data logger is employed to record and process the pressure data. Free surface deformations are observed using a high-speed camera and free surface elevations are compared at each fill level. A high-speed camera (Phantom Micro eX4) is used to track and visualise the free surface profiles at 800 fps. The camera is placed in front of the tank, and an LED lighting panel is placed across from the camera.

Sloshing can create significant impact loads on tank walls depending on the motion and the geometrical parameters. Three different liquid fill levels and various surge excitation frequencies

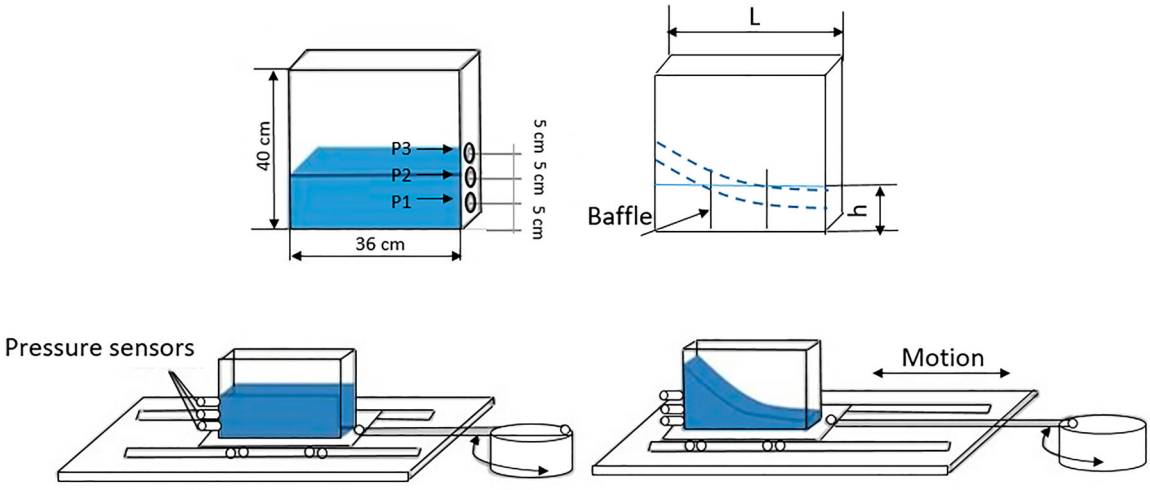

Figure 1. Experimental setup of the surge mechanism. (This figure is available in colour online.)

with a constant amplitude of 11 cm (~L/3) were considered in the experiments. With this amplitude level of excitation, it is ensured that the sloshing motion will be nonlinear. The fill levels are chosen to be 4.5 cm (~H/9), 10.8 cm (~H/3.7) and 14.5 cm (~H/2.75), and named as low, medium and high fill levels, respectively. Pressure sensors are positioned on the side wall at heights corresponding to the three fill levels in order to obtain the pressure values near the calm free surface. The vertical perforated baffles are mounted on the bottom of the tank extending the full width of the tank. The geometrical details and the configuration of baffles are illustrated in Figure 2. Two different configurations are considered to investigate the effect of the number of baffles in damping the sloshing loads. The first one is done by installing one baffle in the middle of the tank, and the second one is done by installing two identical baffles placed at intervals of $L/3$. In order to show the baffle effect on free surface deformations and impact loads, the same excitation frequencies and fill levels are used in the experiments for all cases with and without baffles. The experiments and the recordings were started at the same initial position. For each experiment, 16 cycles were recorded after the dominant oscillation frequency is reached.

When the excitation frequency is close to the natural frequency of the tank, the maximum peak pressure is expected to occur on the side walls. The natural frequency of a narrow rectangular test tank with a length of L and fill level of h can be analytically determined based on the potential flow theory as follows (Faltinsen and Timokha 2009).

$$\omega_n = \sqrt{g\left(\frac{\pi n}{L}\right)\tanh\left(\frac{\pi n}{L}h\right)},\ n = 1, 2, 3.. \tag{1}$$

where n is the mode number. For a narrow rectangular tank with a bottom-centre mounted vertical solid baffle, the first-mode natural frequency can be calculated as follows (Faltinsen and Timokha 2009).

$$\frac{\omega_1'^2}{\omega_1^2} = 1 - \frac{2\pi^2 sin^2(\pi/2)}{\sinh(2\pi h/L)}\left(\frac{h_b}{L}\right)^2 \tag{2}$$

where h_b is the height of the baffle. The lowest natural frequency of the test tank with and without the perforated baffles is shown for each fill level in Table 1. In total, 36 different excitation frequencies are applied in order to determine the natural frequency of the tank with perforated baffles. It is seen in Table 1 that the natural frequency has been shifted due to the presence of the baffles. The natural frequency of the tank with one vertical baffle is found to be lower than the one found without the baffle. Whereas the natural frequency is increased to higher values with the addition of the second baffle.

3. Results and discussion

For a given tank geometry, there are three significant parameters affecting the free surface deformation and the impact pressures in a tank; liquid fill level, surge excitation frequency and its amplitude. In this study, the sloshing tests are carried out with three fill levels of ~H/9, ~H/3.7, ~H/2.75 at 36 different excitation frequencies varying between 2.36 and 8.72 rad/s with a constant surge amplitude of 11 cm (~L/3) covering the on- and off-resonant regions in all cases. Sloshing due to oscillation motion may drive a number of modes in a test tank. The horizontal motion due to surge excitation is defined by the following equation:

$$x(t) = -\xi\cos(\omega t), \quad u(t) = \xi\omega\sin(\omega t) \tag{3}$$

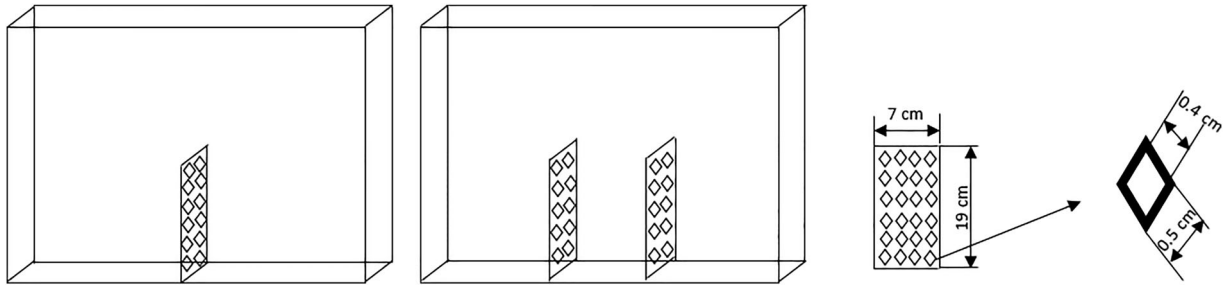

Figure 2. Baffle configurations and their geometrical characteristics.

Table 1. The natural frequencies in the low, medium and high filled cases.

Fill level	Natural Freq. ω_1 (rad/s) no-baffle	Natural Freq. ω_1' (rad/s) one-baffled (Equation (2))	Natural Freq. ω_1' (rad/s) one-baffled (measured)	Natural Freq. ω_1'' (rad/s) two-baffled (measured)
Low	5.65	4.53	5.14	5.32
Medium	7.93	5.3	6.15	7.13
High	8.54	5.95	6.54	7.85

where ξ and ω are amplitude and excitation frequency of the surge motion, respectively. The experiments were carried at excitation frequencies below, above and in the vicinity of the first natural frequency of the test tank.

3.1 Wave generation

When a tank is subjected to surge excitation, water in the tank moves in the opposite direction of the surge motion and hits the side walls because of the inertia of rest. As the bulk water in the tank sloshes with a violent disturbance, the free surface begins to deform and wave elevations occur. The wave shapes are of great importance in pressure variations on the side walls and also alter the magnitude of peak pressures. At smaller amplitudes of surge, the free surface motion remains linear in the off-resonant regions. Increasing the surge amplitude further, the wave elevations grow larger, sloshing becomes more violent and the water climb-ups may hit the roof of the tank leaving the bottom of the tank empty. Therefore, the peak impact pressure has a limit depending on the fill level and the excitation frequencies. At higher fill levels, horizontal and vertical velocity components does not change much in the bottom region of the tank. When a sloshing wave occurs, it propagates towards the sidewall with a horizontal velocity. At the same time, a vertical motion of water is generated on the sidewalls. The wave hits and climbs up on the side wall. Then, the rest of the bulk water moves and hits the side wall. Kisacik et al. (2012) explained a complete wave generation mechanism with different horizontal and vertical water velocities. These differences cause different impact histories on the sidewalls. When the vertical velocity of water surpasses the horizontal velocity, a breaking wave does not occur near the sidewall. Whereas, when the horizontal velocity of water dominates the vertical one, a breaking wave may occur and some air pockets may be observed as well. The size of an air pocket depends on the difference in magnitudes of the horizontal and vertical velocities. The air pockets can produce large pressures on the sidewalls. The location of these air pockets is around the still water level (Wood et al. 2000; Lugni et al. 2006). Later, the air pockets disperse into water during the impact resulting in aerated regions of water. After reaching its peak around the still water level on the sidewall, the pressure decreases, and the moving water loses its initial energy. Therefore, less impact pressures are measured on the other parts of the sidewall. The free surface can rise up on the sidewalls as much as its initial energy. Figure 3 shows some high-speed images taken at the excitation frequencies of 0.78 and 0.84 ω_1. Figures 3a and 3b represent non-breaking and breaking wave impacts, respectively. It can be seen from these images that wave breaking occurs near the side wall. Breaking waves are only observed at frequencies close to the first-mode natural frequency, ω_1 of the tank.

3.2 Free surface deformation

The way the sloshing waves evolve is also crucial in a sloshing event because the free surface deformation is related to the rate of water oscillation in the tank. The displacement of water during a sloshing event as a function of fill level and natural frequency of tank. Figure 4 illustrates the free surface deformations obtained during one cycle of water motion in three fill levels at the excitation frequency of 6.68 rad/s. The distance values, z and x are normalised by the fill level and the tank length, respectively, i.e. $z^* = z/h$ and $x^* = x/L$.

The water fill level modifies the natural frequency of the tank. Larger free surface deformations are expected to occur when the excitation frequency gets closer to the tank's natural frequency. Therefore, while higher free surface deformations are observed in the low and medium fill levels, less deformation occurs in the high fill level under the same excitation conditions due to being in the non-resonance region. It can be seen in Figure 4 that the maximum normalised climb-up height on the sidewall in the low fill level is 4.5, whereas this value decreases to 3 and 2.5 in the medium and high fill levels, respectively.

Figure 5 illustrates the free surface deformations at the end of one surge motion obtained at various frequencies. At 5.34 rad/s, the water climbs up on the side wall to a height 30% higher than the one at 4.78 rad/s frequency in the low fill level (Figure 5a). Whereas the difference between the max. relative heights (z^*) at 5.34 and 6.68 rad/s frequencies is much larger. Free surface deformations get smaller in the medium and high fill levels (Figure 5b

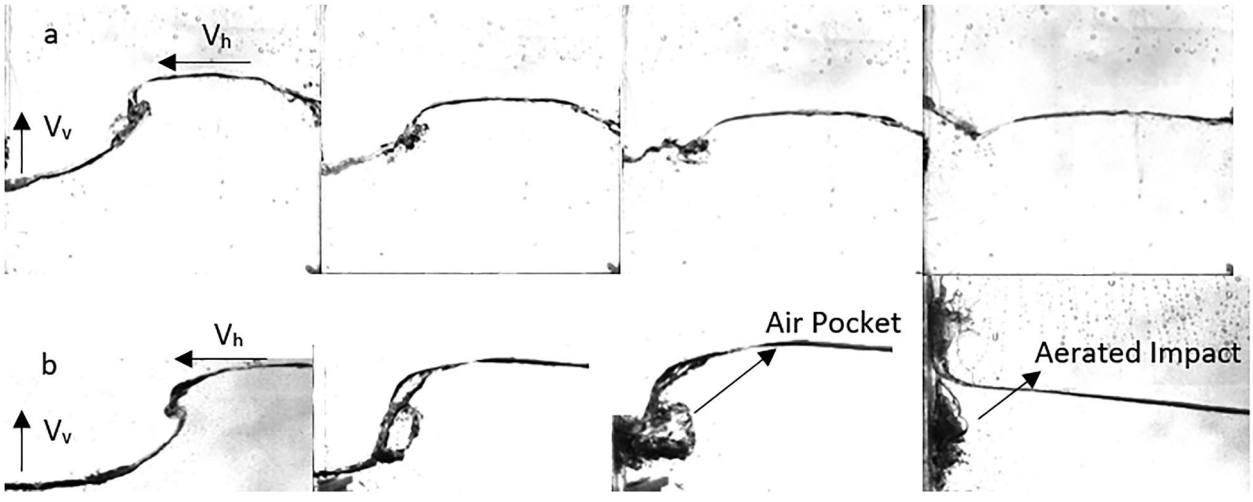

Figure 3. The process of wave generation: (a) $V_h/V_v = 1$ and (b) $V_h/V_v = 5.6$.

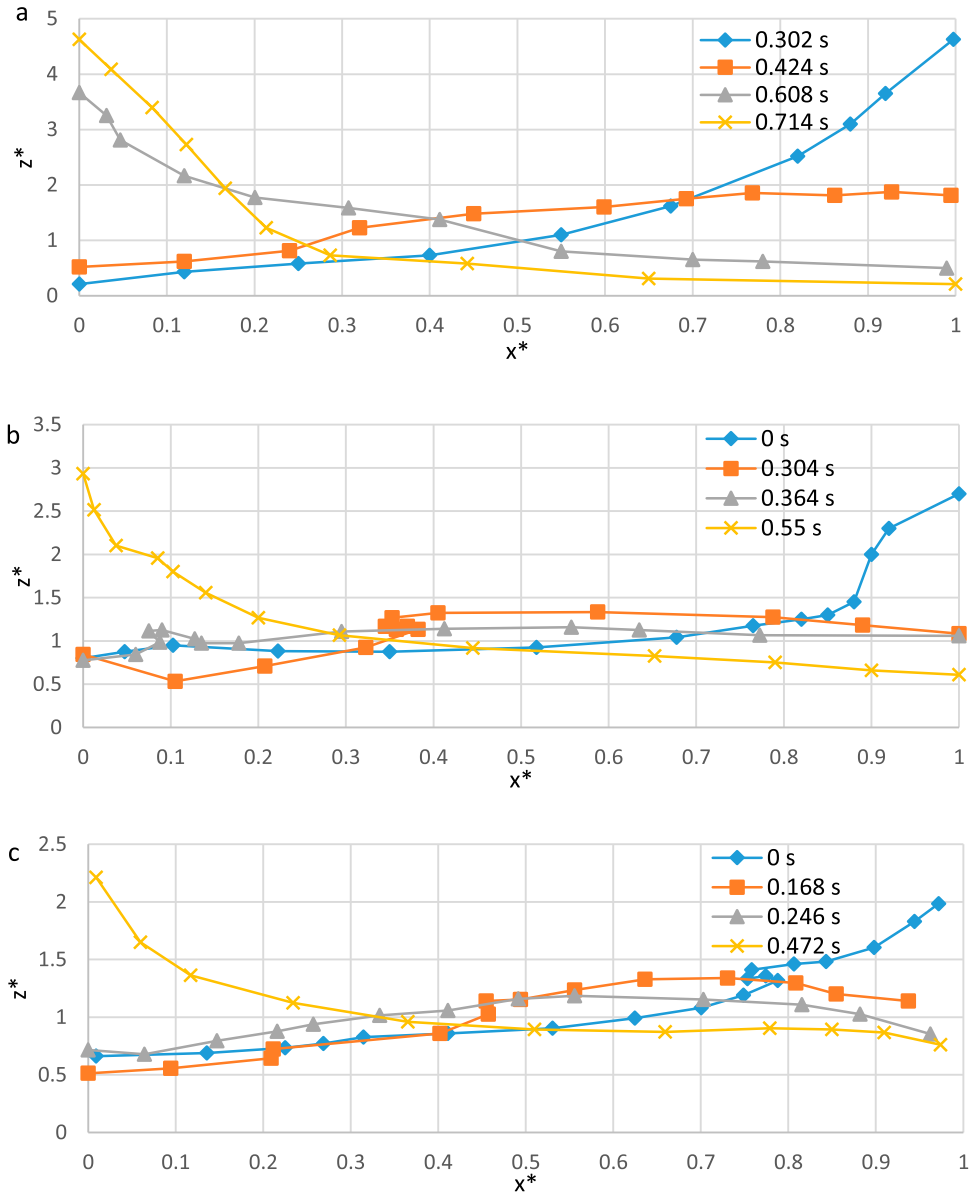

Figure 4. Free surface profiles at various time instants at the frequency oscillation of 6.68 rad/s in the low[a], medium[b] and high[c] water fill levels. (This figure is available in colour online.)

and c), i.e. the effect of excitation frequency on free surface deformation and water climb up decreases with increasing fill level for a given excitation frequency. This indicates that more relative displacement of water occurs in the low fill level for a given excitation frequency.

3.3 Pressure distribution on the side wall

The pressure measurements were carried out via three pressure sensors located at the heights corresponding to the three fill levels. Identical tests for each excitation frequency were carried out to ensure the repeatability of the experiments. The repeatability of the pressure measurements is observed under the same test conditions and shown in Figure 6 for high fill levels. Figure 6 shows the pressure measurements obtained using two different pressure transducers mounted at the same elevation on the wall.

For the pressure measurements, the same excitation frequencies with a fixed amplitude of 11 cm have been induced in all fill levels. The time histories of the pressure values normalised by $\rho^{*}g^{*}L$ (where ρ is the density, g is the gravity and L is the length of tank) are shown for 16 cycles in Figure 7. After each impact, pressure values drop down to a value near zero. Impact pressures increase with increasing fill level (Figure 7). However, shock pressures may be much larger than the impact pressures (Figure 7b). It is seen that the location of the peak pressure corresponds to the height of the calm free surface. This means that the maximum impact force occurs on the wall near the calm free surface level where the sloshing waves are generated. The relation between the fill level and the pressure on the side wall is linear at this excitation level. When the excitation frequency is in the vicinity of the lowest natural frequency of the tank, violent sloshing is observed, i.e. shock pressures are detected in terms of large peaks. The fluid behaviour is not the same at each cycle due to the nonlinearity (Wei et al. 2015). Similar pressure–time histories have been reported by others (Kisacik et al. 2012; Wei et al. 2015; Lugni et al. 2010b). Primary wave and the reflected wave interaction, air cushioning effect and turbulence after the breaking wave may be the reason for these non-symmetrical pressure histories (Kisacik et al. 2012). The magnitudes of these

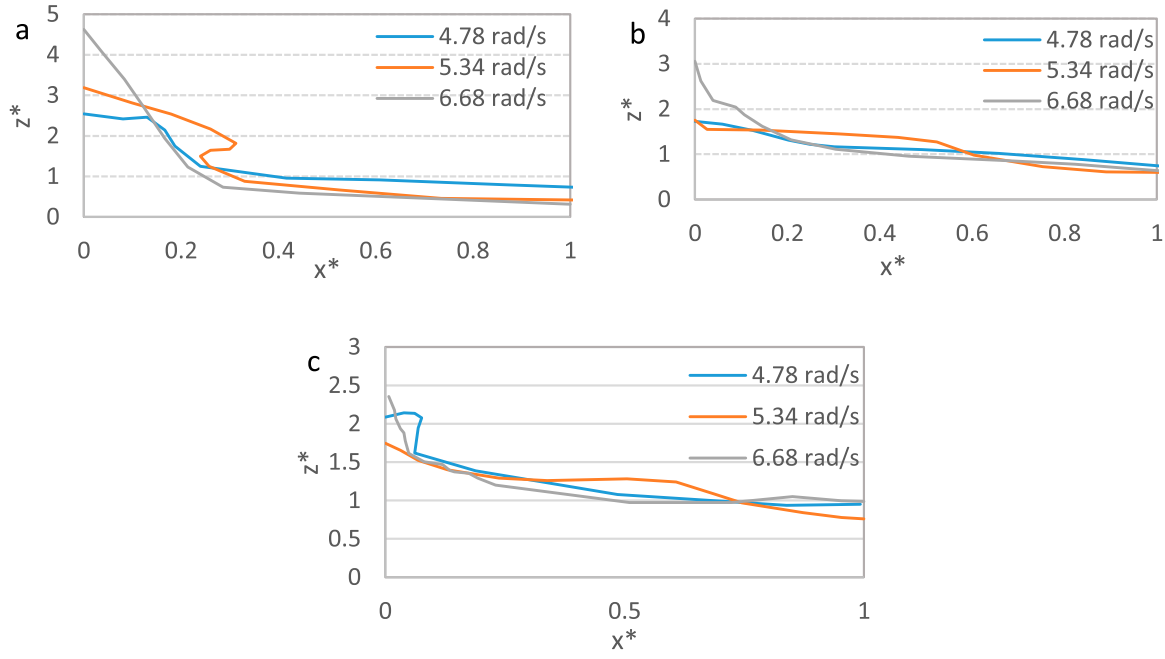

Figure 5. Free surface profiles at the end of one sway motion in low[a], medium[b] and high[c] fill levels at various excitation frequencies. (This figure is available in colour online.)

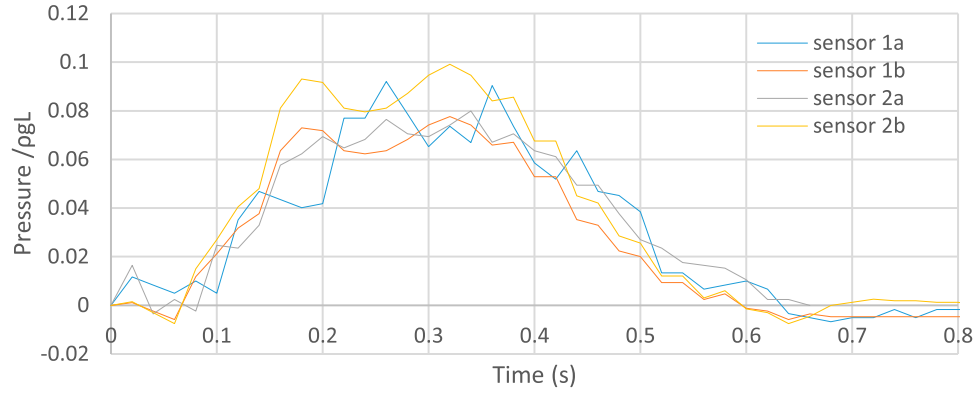

Figure 6. Repeatability of the sloshing tests in high fill levels. Pressure values measured with two different pressure sensors at the same elevation at 4.68 rad/s. (This figure is available in colour online.)

peaks are not the same in each cycle. Strong sloshing-induced shock pressures are recorded in the low and medium fill levels by the first and second pressure sensors, respectively (Figure 7a and 7b) due to the excitation frequency being close to the natural frequency of the tank at this fill levels. However, in the high fill level, no significant shock pressure is captured by any sensor due to the higher natural frequency (Lugni et al. 2010b).

Figure 8 shows the snapshots of the free surface profiles taken during the sloshing tests in each fill level at the frequency of 6.68 rad/s. The aerated water impact is observed in the low and medium fill levels (Figure 8a, 8b). Whereas there is no air–water mixture impact acting on the side wall in the high fill level. An air pocket is observed before the impact in the medium fill level, then it disappears around the second sensor location (Figure 8b). There is a minimum amount of aeration in the high fill level.

Figure 9 shows the normalised pressure values recorded during one cycle in each fill level at the same excitation frequency. The normalised values of pressure appear to scale up as the fill level increases up to a limit value. In higher fill levels, surge motion energy is conserved within the higher amount of water, i.e. less movement of water in the tank. During a sloshing impact, the pressure reaches its peak value at the beginning of the impact in low fill levels. However, some oscillations in pressure may be observed before the peak in higher fill levels. A second peak is also detected in all fill levels due to gravity. After the first peak, while the wave comes down and hits the bulk water, i.e. backflow, a second peak is observed at all pressure sensors (Zou et al. 2015). Some negative values of pressure are detected at the beginning of the impact due to the vertical water flow passing by the sensors and rapidly rising at high velocities, i.e. violent sloshing (Hattori et al. (1994)). However, negative pressure values are not observed in the high fill level because of the non-existence of high velocity water flow along the side walls.

The pressure–time histories measured by the first pressure sensor (P1) in all fill levels are compared in Figure 10. While the time the peak pressure value is reached is 0.04 s in the low fill level, it is measured as 0.18 and 0.26 s in the medium and high fill levels, respectively.

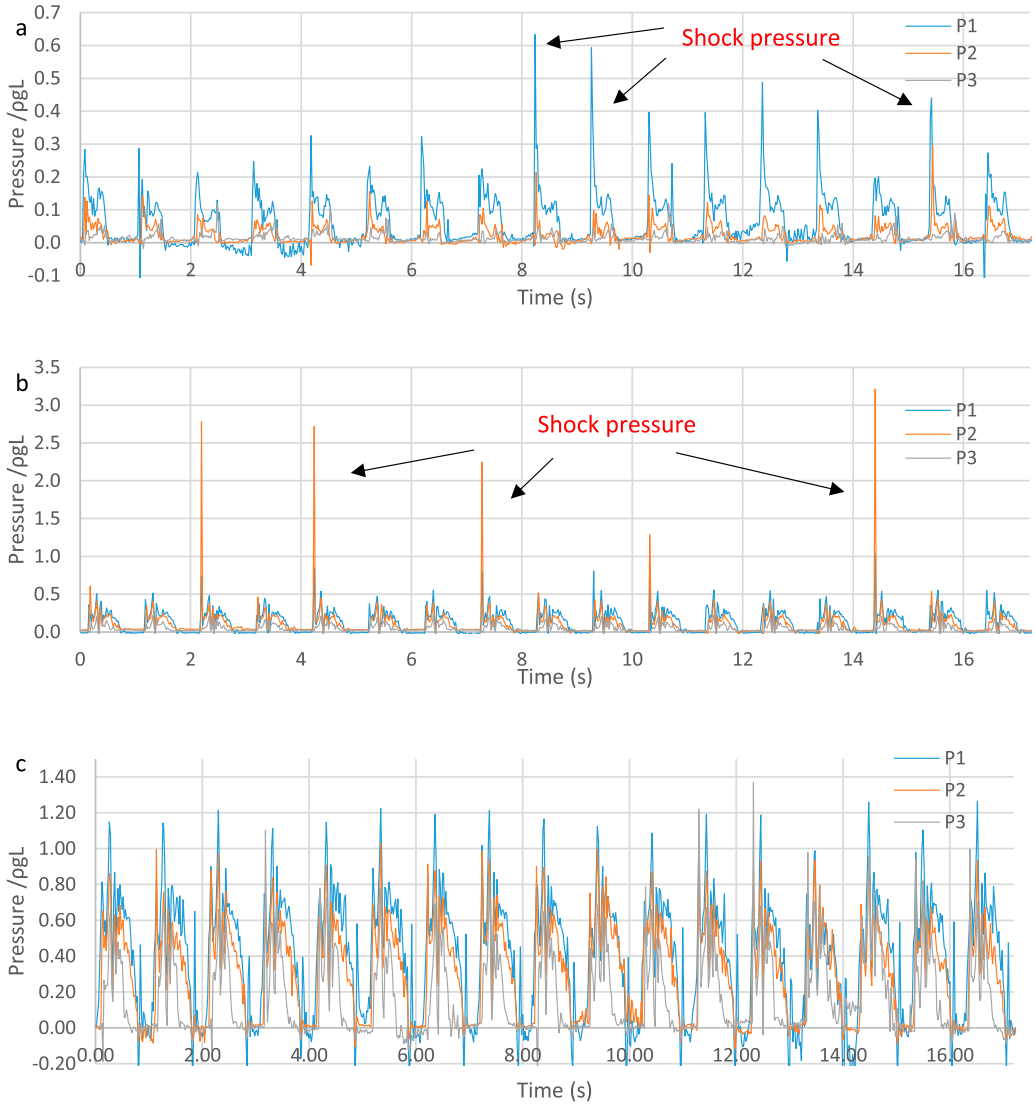

Figure 7. Pressure-time histories obtained by three pressure sensors in low[a], medium[b] and high[c] fill levels at the oscillation frequency of 6.68 rad/s. (This figure is available in colour online.)

3.4 The effect of baffles

In this section, single and dual perforated baffles are considered to investigate the effect of the number of baffles in damping out the sloshing loads and mitigating the fluid motion, i.e. vortex-induced damping. Minimising the number of baffles is of great importance in weight minimisation, fast loading and unloading, and also easy cleaning processes.

For the sake of comparison, the same fill levels and excitation frequencies are applied as in the no-baffle case. Each perforated baffle has the same dimensions and solidity ratios. One baffle is installed in the middle of the tank in the one-baffle case, and two identical baffles are installed with equal spacing between the baffles and the tank walls in the two-baffle case. The free surface elevations and peak pressure values are compared between the cases. Table 1 compares the natural frequency of the test tank with and without the baffles in all three fill levels. The natural frequencies of the tank with one and two baffles are 10–25% and 5–10% less than those of the tank without baffle, respectively.

Figure 11 compares the free surface profiles in all three cases in the low fill level during one excitation cycle. In this fill level, violent water movement was observed in the no-baffle case. On the other hand, in the cases with baffles, the baffles considerably reduced the water movement in the test tank which indicates that baffles can damp out the kinetic energy of the sloshing waves and prevent strong waves from hitting the sidewalls with high climb ups.

Figure 12 presents the high-speed images taken at the end of one sway motion in all three cases in the low fill level at the frequency of 5.34 rad/s. While the sloshing wave floods to the left side and climbs up high in the no-baffle case, the wave amplitudes get smaller in the one- and two-baffle cases. The perforated baffles dissipate the kinetic energy of the waves through the viscous effects and damp out the sloshing loads. Therefore, less water run-ups were observed and more stable fluid distribution in the tank was achieved with the baffles. It can be seen from Figure 12 that there is no overturning flow from the side wall in the baffle cases.

From the high-speed images taken at the end of one sway motion, Figure 13 demonstrates the water run-up levels in no-, one- and two-baffle cases at two excitation frequencies in all fill levels. The rise of the free surface on the sidewall may reach to the roof of the tank in the low fill level in no-baffle case (Figure 13a). The effect of the baffles in mitigating the fluid flow is stronger in low fill levels. However, the second baffle effect is not significant in the high fill level (Figure 13c). In order to show the damping ratio of wave elevation,

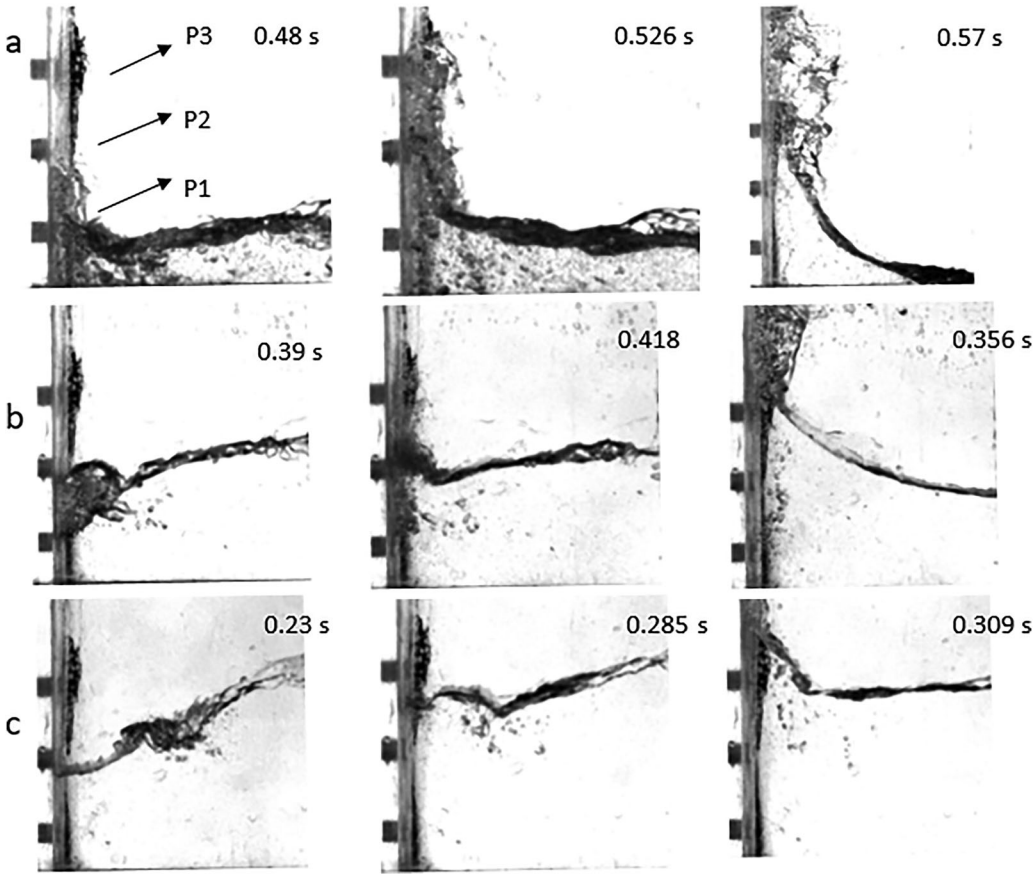

Figure 8. Snapshots taken at various time instants during the wave impacts in low[a], medium[b] and high[c] fill levels.

Cho and Kim (2016) introduced an amplification factor as

$$Rn = \frac{\eta_{max} - \eta_{min}}{2\xi} \tag{4}$$

where ξ is the sway amplitude and η is the wave elevation.

Stronger damping is observed under baffle effects in the low fill level at all excitation frequencies. The reduction rate in the amplification factor (R_n) between the cases of no-baffle and two-baffle is about 60% at the oscillation frequency of 5.34 rad/s. And this reduction rate decreases to 48% when comparing to the one-

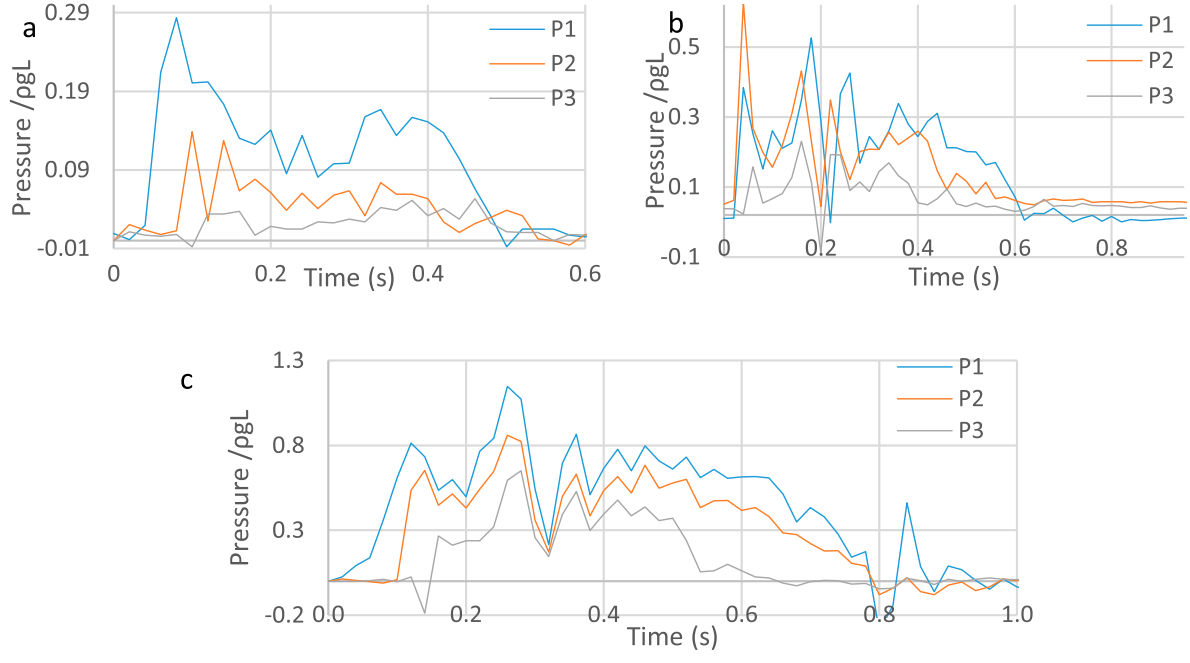

Figure 9. Pressure-time histories in low[a], medium[b] and high[c] fill levels at the oscillation frequency of 6.68 rad/s. (This figure is available in colour online.)

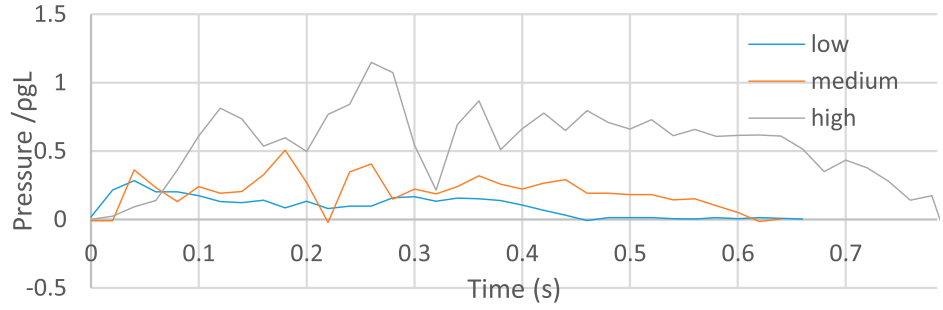

Figure 10. The pressure-time histories (P1) in three fill levels at the oscillation frequency of 6.68 rad/s. (This figure is available in colour online.)

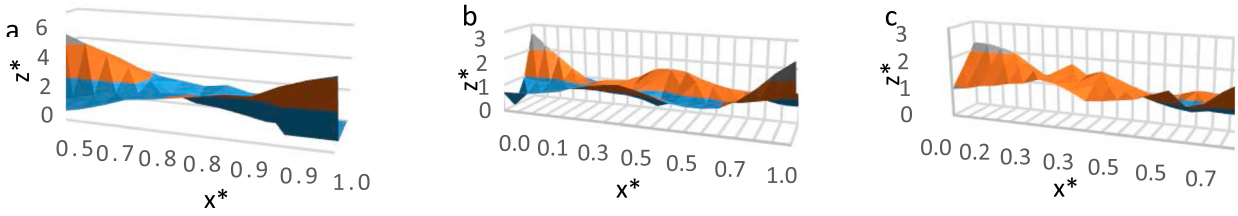

Figure 11. Free surface profiles in no baffle[a], one-baffle[b], and two-baffle[c] cases in the low fill level at the frequency of 5.34 rad/s. (This figure is available in colour online.)

baffle case. However, these rates are smaller in the medium fill level, i.e. 45–35%, respectively. Furthermore, the benefit of installing the second baffle disappeared in the high fill level giving the reduction rates of 18–16% in two- and one-baffle cases, respectively. One-baffle installation already resulted in a remarkable suppression of the wave elevation along the sidewall at these frequency levels.

The pressure–time histories over 16 cycles in the one- and two-baffle cases are presented in the low and medium fill levels in Figures 14 and 15, respectively. More symmetrical pressure profiles are observed in each cycle in the cases with baffles. The peak pressure values increase with increasing excitation frequencies in the no-baffle case when the frequency is less than the first-mode natural frequency. The peak pressure values in all cases in the high fill level are plotted as a function of the excitation frequency in Figure 16. It can be seen in Figure 16 that the baffles not only significantly decrease the peak magnitudes of sloshing loads but also shift the resonance frequencies to lower levels (Figure 16b, c). As the oscillation frequencies get nearer the resonance region, the damping effect of the baffles becomes much stronger, whereas the reduction in sloshing loads due to baffles is smaller at non-resonance frequencies. Since the natural frequency is shifted to a lower value with the addition of a baffle, sloshing loads is decreased further at higher frequencies and to even much lower values at the natural frequency of the tank without baffle. With the addition of the second baffle, the natural frequency is shifted to a higher value but smaller than the one with no-baffle case, and yet the reduction in sloshing loads is at the same level as in one-baffle case. Due to the resonance frequency shifted to lower values with baffles, shock impact pressures are rarely observed in any fill level, similar to the findings of Wei et al. 2015; Faltinsen and Timokha 2011; Akyildiz and Ünal 2005. When one or two baffles are added, the peak pressure is reduced by 70% compared to the no-baffle case at the frequencies near the natural frequency of the tank.

For a given oscillation frequency, the peak pressure values are measured with an uncertainty of ±1–3% on average. However, higher level of uncertainties may arise around the resonance frequency due to high nonlinearity.

Figure 17 shows the pressure–time histories during one cycle in all three cases in the low fill level. The duration of the impact on the sidewall is shorter in the baffled cases compared to the no-baffle case. The characteristics of the pressure–time histories are also different in the baffled cases. The peak pressure is delayed in the one-baffle case due to energy losses of the sloshing waves and therefore delayed the water impact on the side wall. The second baffle decreases the wave energy further, therefore a significant peak pressure is not observed in the two-baffle case.

Figure 18 demonstrates how the effect of baffles in suppressing sloshing is altered with the excitation frequency. The damping ratio is increased with increasing excitation frequency due to getting closer to the resonance level.

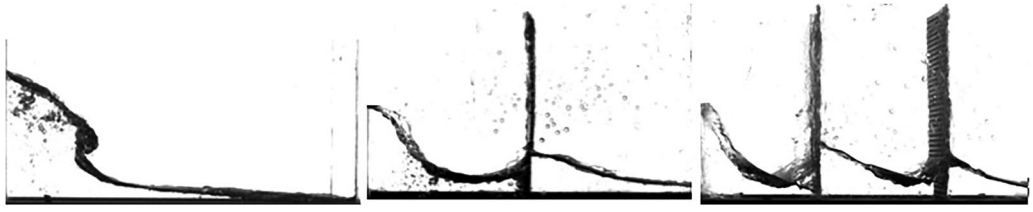

Figure 12. The free surface profiles at the end of one sway motion in no-, one-, and two-baffle cases in the low fill level at the frequency of 5.34 rad/s.

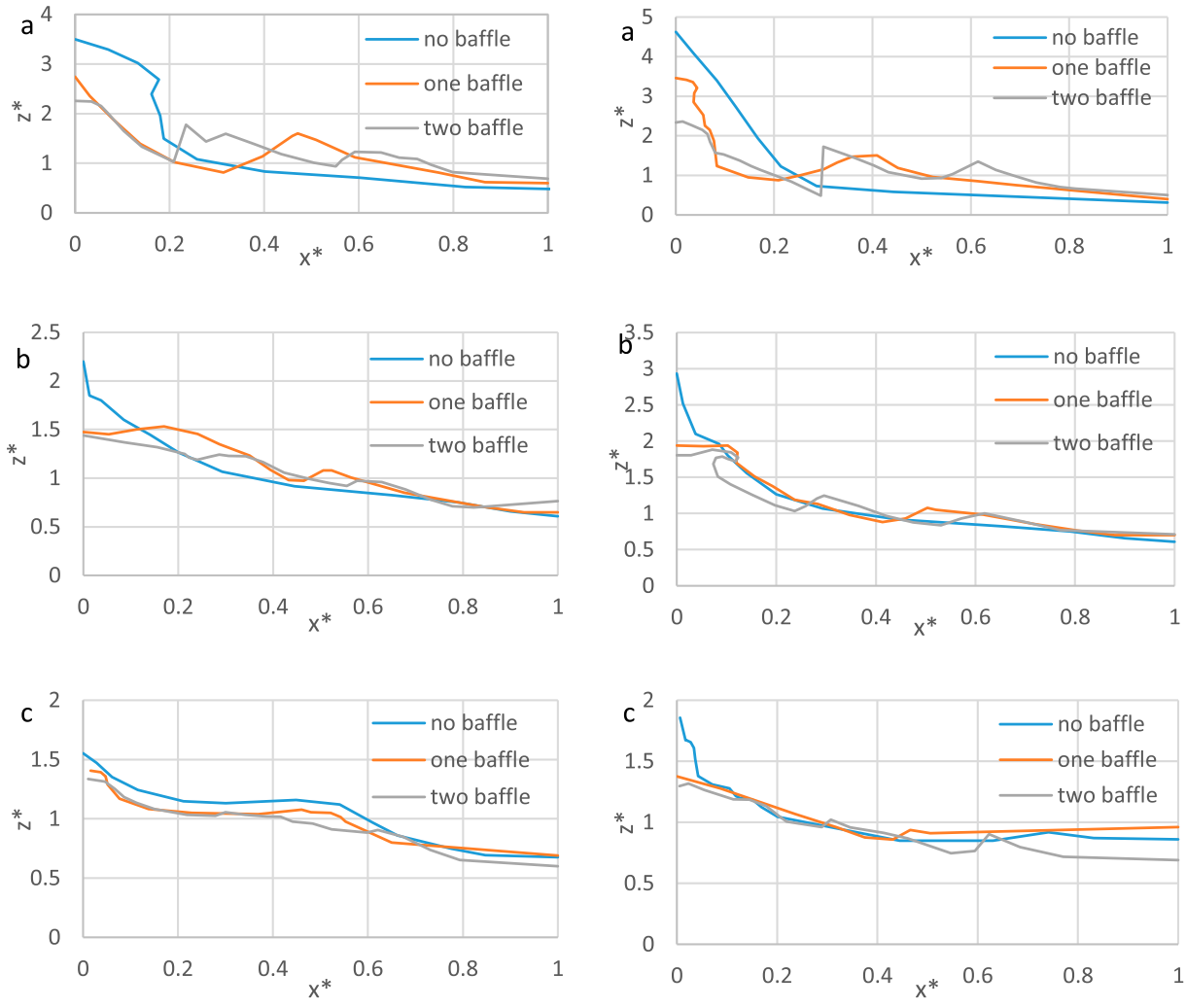

Figure 13. The free surface profiles in the low[a], medium[b] and high[c] fill levels at the oscillation frequencies of 5.34 rad/s (left) and 6.68 rad/s (right). (This figure is available in colour online.)

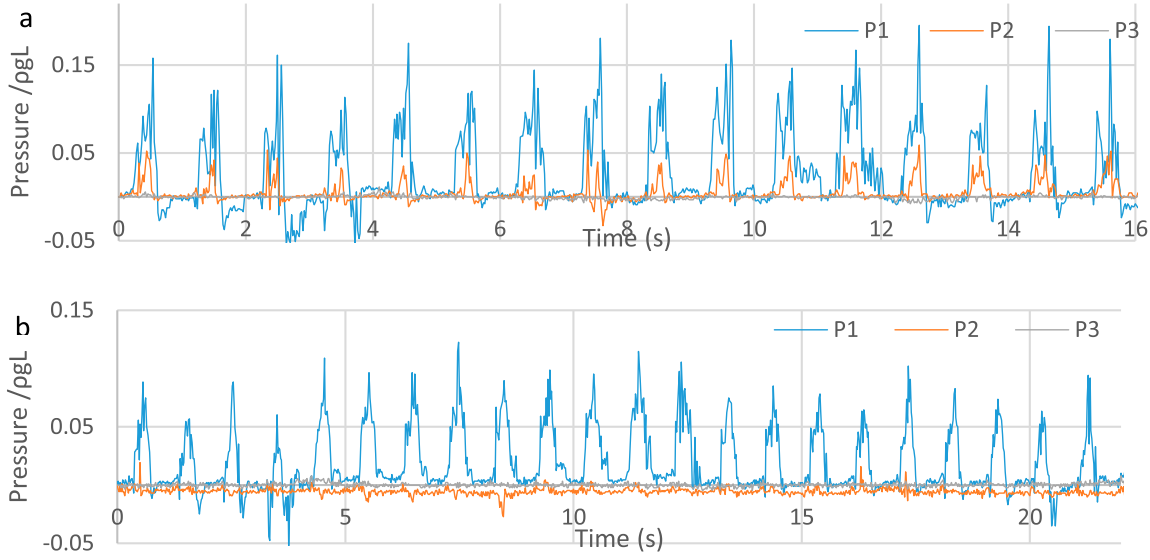

Figure 14. Pressure-time histories in one-[a] and two-[b] baffle cases in the low fill level at the oscillation frequency of 6.68 rad/s. (This figure is available in colour online.)

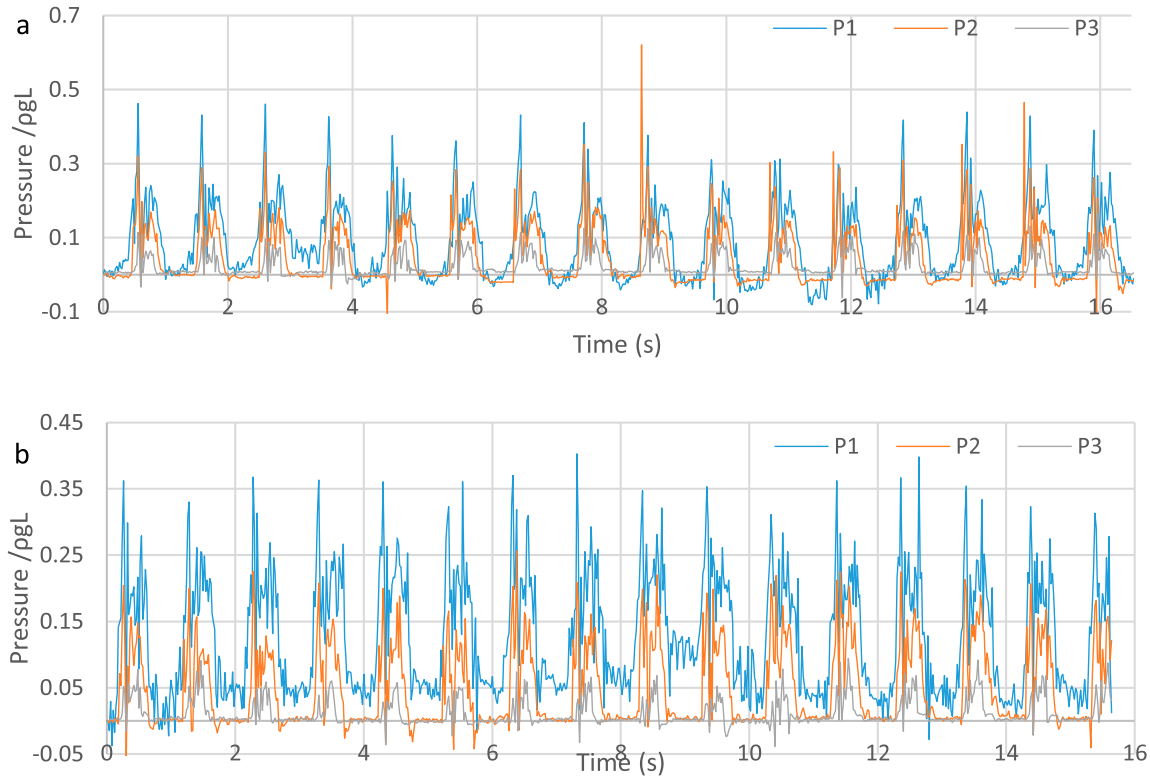

Figure 15. Pressure-time histories in one-[a] and two-[b] baffle cases in the medium fill level at the oscillation frequency of 6.68 rad/s. (This figure is available in colour online.)

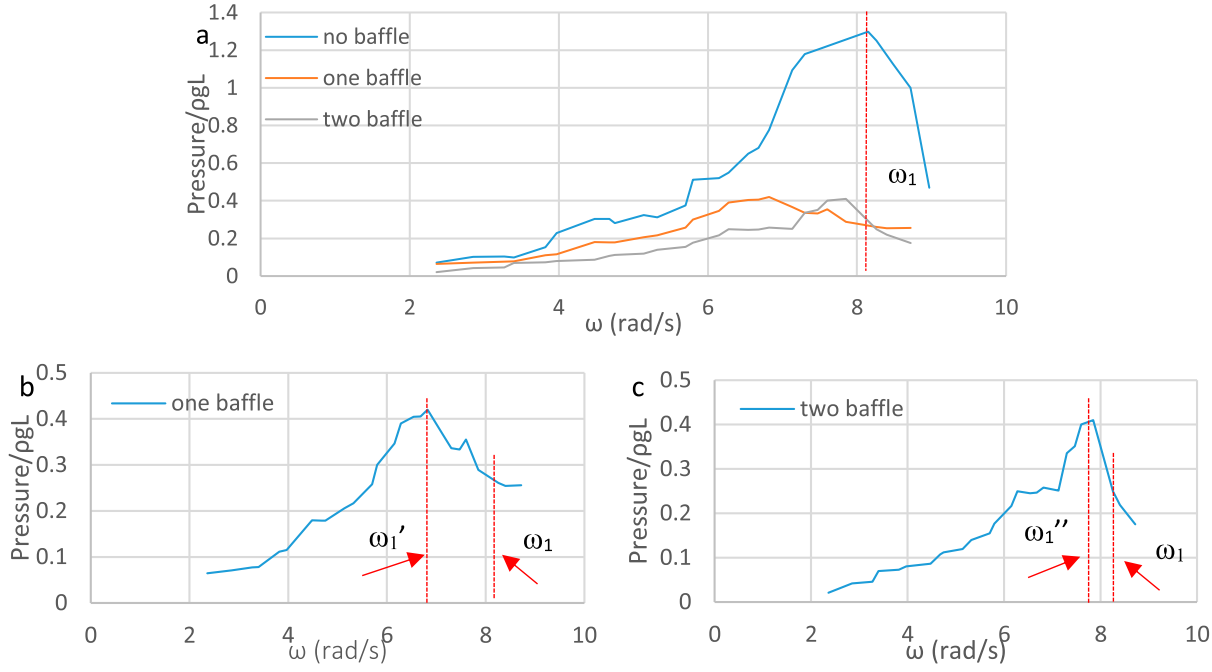

Figure 16. Peak pressure vs. the excitation frequency in all cases in the high fill level. (This figure is available in colour online.)

Table 2 shows the damping effects of the perforated baffles on the peak pressure values in all fill levels. Significant decreases are observed in the low fill level, e.g. 26% with one baffle. The second perforated baffle is useful in mitigating the sloshing effects in the low fill level, i.e. 45% reduction in the vicinity of the resonance frequency. However, the damping effect of baffles in reducing the peak pressure is less significant in the medium and high fill levels due to being in the off-resonant region. The second baffle in particular has a minor effect in the medium and high fill levels indicating that the use of a second baffle is ineffective and unnecessary at this frequency levels.

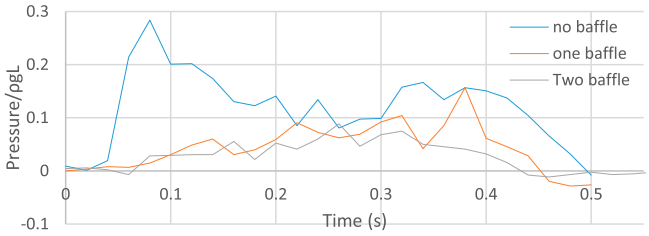

Figure 17. Pressure–time histories in all cases in the low fill level at the oscillation frequency of 6.68 rad/s. (This figure is available in colour online.)

Table 2. The normalised peak pressure values measured at the calm water levels in no-, one-, and two-baffle cases in all fill levels at 3.4 rad/s.

	Low filled	Medium filled	High filled
No-baffle	0.078	0.147	0.098
One-baffle	0.058	0.12	0.078
Two-baffle	0.043	0.111	0.07

4. Conclusion

In this study, the effect of the number of perforated baffles in damping the sloshing loads is experimentally investigated in a rectangular tank by examining the free surface profiles and the pressure–time histories on the side wall in three different fill levels. The following conclusion can be drawn from this study:

The rate of free surface deformation of the horizontally oscillating water is higher at the excitation frequencies near the natural frequency of the tank which varies with the liquid fill level. Self-damping effects are stronger in the off-resonant regions in all fill levels. Therefore, sloshing loads are lower in off-resonant regions.

Using perforated baffles in a tank dissipates the kinetic energy of sloshing waves, suppresses the water motion in the tank, significantly reduces the pressure loads acting on the side walls, and shifts the tank's natural frequency. Baffles restrain the liquid displacement in a tank causing much less violent sloshing and more homogenous free surface profiles.

Using a single perforated baffle is already quite effective in suppressing sloshing and reducing the impact loads. Therefore, introducing a second baffle is ineffective particularly in higher fill levels and at some frequencies. However, it significantly reduces the impact loads when the oscillation frequency is near the natural frequency of the tank with one baffle. These results indicate that the second baffle does not contribute much in suppressing the sloshing loads in the off-resonant regions, but causes to change the natural frequency of the tank.

It is suggested that the number of baffles to be installed on a liquid cargo ship can be minimised while still performing the necessary amount of damping depending on the excitation frequency and the natural frequency of the ship. For weight and

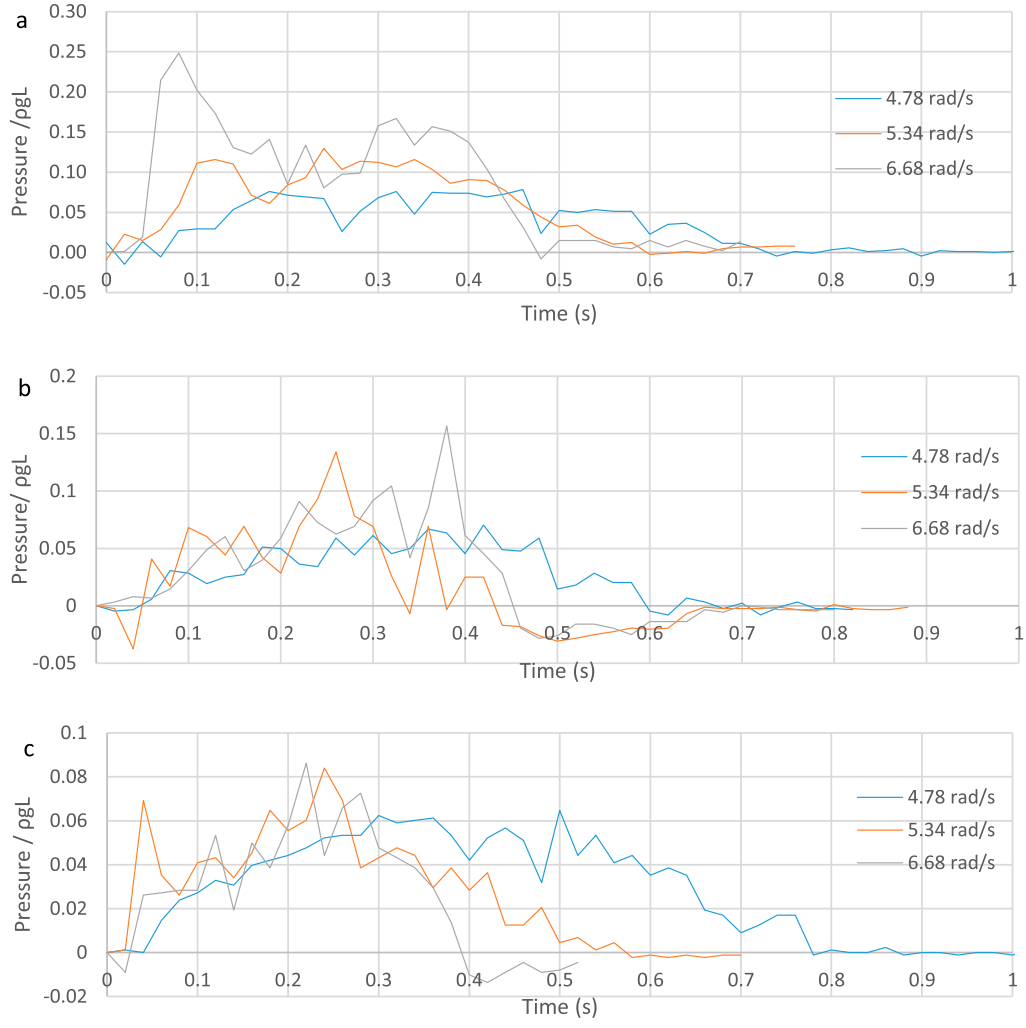

Figure 18. Pressure-time histories of P1 in the low fill level case with no[a], one[b] and two[c] baffles at various oscillation frequencies. (This figure is available in colour online.)

cost minimisation, fast loading and unloading, and easy cleaning processes, the determination of the baffle arrangement with minimum number and weight can be obtained in model tests and/or numerical simulations for liquid cargo carriers.

Disclosure statement

No potential conflict of interest was reported by the author(s).

Funding

This research has been financially supported by Yildiz Technical University Research Grants (Grant FBA-2018-3341).

ORCID

Fatih C. Korkmaz http://orcid.org/0000-0001-9250-5265
Bülent Güzel http://orcid.org/0000-0001-6915-4209

References

Akyildiz H, Ünal E. 2005. Experimental investigation of pressure distribution on a rectangular tank due to the liquid sloshing. Ocean Eng. 32:1503–1516.
Bellezi CA, Cheng LY, Okada T, Arai M. 2019. Optimized perforated bulkhead for sloshing mitigation and control. Ocean Eng. 187:106171.
Bouscasse B, Antuono M, Colagrossi A, Lugni C. 2013. Numerical and experimental investigation of nonlinear shallow water sloshing. Int J Nonlinear Sci Numer Simul. 14:123–138.
Brizzolara S, Savio L, Viviani M, Chen Y, Temarel P, Couty N, Hoflack S, Diebold L, Moirod N, Iglesias AS. 2011. Comparison of experimental and numerical sloshing loads in partially filled tanks. Ships Offsh Struct. 6(1–2):15–43.
Bullock GN, Obhrai C, Peregrine DH, Bredmose H. 2007. Violent breaking wave impacts. part 1: results from large-scale regular wave tests on vertical and sloping walls. Coastal Eng. 54:602–617.
Cho IH, Kim MH. 2016. Effect of dual vertical porous baffles on sloshing reduction in a swaying rectangular tank. Ocean Eng. 126:364–373.
Colagrossi A, Palladino F, Greco M, Lugni C, Faltinsen OM. 2004. Experimental and numerical investigation of 2D sloshing: scenarios near the critical filling depth. In: Proc. 19th International Workshop on Water Waves and Floating Body; March 28–31; Cortona, Italy.
Crowley S, Porter R. 2012a. An analysis of screen arrangements for a tuned liquid damper. J Fluids Struct. 34:291–309.
Crowley S, Porter R. 2012b. The effect of slatted screens on waves. J Eng Math. 76:33–57.
Faltinsen OM, Timokha AN. 2009. Sloshing. New York: Cambridge University Press.
Faltinsen OM, Timokha AN. 2011. Natural sloshing frequencies and modes in a rectangular tank with a slat-type screen. J Sound Vib. 330:1490–1503.
Goudarzi MA, Sabbagh Yazdi SR, Marx W. 2010. Investigation of sloshing damping in baffled rectangular tanks subjected to the dynamic excitation. Bull Earthquake Eng. 8:1055–1072.
Graczyk M, Moan T, Wu MK. 2007. Extreme sloshing and whipping-induced pressures and structural response in membrane LNG tanks. Ships Offsh Struct. 2(3):201–216.
Hattori M, Arami A, Yui T. 1994. Wave impact pressure on vertical walls under breaking waves of various types. Coastal Eng. 22(Special Issue Vertical Breakwaters):79–114.
Kim SY, Kim Y, Lee J. 2017. Comparison of sloshing-induced pressure in different scale tanks. Ships Offsh Struct. 12(2):244–261.
Kisacik D, Troch P, Van Bogaert P. 2012. Description of loading conditions due to violent wave impacts on a vertical structure with an overhanging horizontal cantilever slab. Coastal Eng. 60:201–226.
Liu D, Lin P. 2009. Three-dimensional liquid sloshing in a tank with baffles. Ocean Eng. 36:202–212.
Lu Y, Zhou T, Cheng L, Zhao W, Jiang H. 2018. Dependence of critical filling level on excitation amplitude in a rectangular sloshing tank. Ocean Eng. 156:500–511.
Lugni C, Brocchini M, Faltinsen OM. 2006. Wave impact loads: The role of the flip-through. Phys Fluids. 18:122101.
Lugni C, Brocchini M, Faltinsen OM. 2010a. Evolution of the air cavity during a depressurized wave impact. II. The dynamic field. Phys Fluids. 22:056102.
Lugni C, Miozzi M, Brocchini M, Faltinsen OM. 2010b. Evolution of the air cavity during a depressurized wave impact. I. The kinematic flow field. Phys Fluids. 22:056101.
Maleki A, Ziyaeifar M. 2008. Sloshing damping in cylindrical liquid storage tanks with baffles. J Sound Vib. 311:372–385.
Nasar T, Sannasiraj SA, Sundar V. 2008. Sloshing pressure variation in a barge carrying tank. Ships Offsh Struct. 3(3):185–203.
Nasar T, Sannasiraj SA, Sundar V. 2021. Performance assessment of porous baffle on liquid sloshing dynamics in a barge carrying liquid tank. Ships Offsh Struct. 16(7):773–786.
Pistani F, Thiagarajan K. 2012. Experimental measurements and data analysis of the impact pressures in a sloshing experiment. Ocean Eng. 52:60–74.
Rajasekaran C, Sannasiraj SA, Sundar V. 2010. Breaking wave impact pressure on a vertical wall. Int J Ocean Climate Syst. 1:155–166.
Sauret A, Boulogne F, Cappello J, Dressaire E, Stone HA. 2015. Damping of liquid sloshing by foams. Phys Fluids. 27:022103.
Shamsoddini R, Abolpur B. 2019. Investigation of the effects of baffles on the shallow water sloshing in a rectangular tank using A 2D turbulent ISPH method. China Ocean Eng. 33:94–102.
Shamsoddini R, Abolpur B. 2021. Bingham fluid sloshing phenomenon modelling and investigating in a rectangular tank using SPH method. Ships Offsh Struct. 16(5):557–566.
Song YK, Chang KA, Ryu Y, Kwon SH. 2013. Experimental study on flow kinematics and impact pressure in liquid sloshing. Exp in Fluids. 54:1592.
Souto-Iglesias A, Bulian G, Botia-Vera E. 2015. A set of canonical problems in sloshing. Part 2: influence of tank width on impact pressure statistics in regular forced angular motion. Ocean Eng. 105:136–159.
Tosun U, Aghazadeh R, Sert C, Ozer M. 2017. Tracking free surface and estimating sloshing force using image processing. Exp Therm Fluid Sci. 88:423–433.
Wei ZJ, Faltinsen OM, Lugni C, Yue QJ. 2015. Sloshing-induced slamming in screen-equipped rectangular tanks in shallow-water conditions. Phys Fluids. 27:032104.
Wood DJ, Peregrine D H, Bruce T. 2000. Wave impact on a wall using pressure-impulse theory. I: Trapped air. J Waterway Port Coastal Ocean Eng. 126:182–190.
Wu CH, Faltinsen OM, Chen BF. 2013. Analysis on shift of nature modes of liquid sloshing in a 3D tank subjected to oblique horizontal ground motions with damping devices. Adv Mech Eng. 5:1–24.
Xue MA, Chen Y, Zheng J, Qian L, Yuan X. 2019. Fluid dynamics analysis of sloshing pressure distribution in storage vessels of different shapes. Ocean Eng. 192:106582.
Xue MA, Zhenga J, Lind P, Yuan X. 2017. Experimental study on vertical baffles of different configurations in suppressing sloshing pressure. Ocean Eng. 136:178–189.
Yu YM, Ma N, Fan SM, Gu XC. 2017. Experimental and numerical studies on sloshing in a membrane-type LNG tank with two floating plates. Ocean Eng. 129:217–227.
Yu YM, Ma N, Fan SM, Gu XC. 2019. Experimental studies of suppressing effectiveness on sloshing with two perforated floating plates. Int J Naval Archit Ocean Eng. 11:285–293.
Zou CF, Wang DY, Cai ZH, Li Z. 2015. The effect of liquid viscosity on sloshing characteristics. J Mar Sci Technol. 20:765–775.